RNA (2000), *6*:1413–1422. Cambridge University Press. Printed in the USA.
Copyright © 2000 RNA Society.

The 3′ substrate determinants for the catalytic efficiency of the *Bacillus subtilis* RNase P holoenzyme suggest autolytic processing of the RNase P RNA in vivo

ANDREW LORIA and TAO PAN

Department of Biochemistry and Molecular Biology, University of Chicago, Chicago, Illinois 60637, USA

ABSTRACT

We investigated the catalytic efficiency and the specificity of the *Bacillus subtilis* RNase P holoenzyme reaction with substrates that contain a single strand, a hairpin loop, or a tRNA 3′ to the cleavage site. At a saturating ribozyme concentration, RNase P can cleave a single-stranded RNA at ~0.6 min^{-1} at pH 7.8. Replacing the single-stranded RNA 3′ to the cleavage site by a hairpin loop or by the yeast $tRNA^{Phe}$ increases the cleavage rate by up to ~600-fold and ~3,200-fold, respectively. These results show that compared to a single-stranded RNA substrate, the cleavage rate for the holoenzyme reaction is primarily enhanced by an acceptor-stem-like helix. Substrate binding, ~7–10 μM for a single-stranded RNA, improves by ~1,000-fold upon the addition of the tRNA. The efficiency of the RNase P holoenzyme cleaving a single-stranded RNA is sufficiently high to consider autolytic processing of the RNase P RNA (denoted P RNA) transcript in the cell. The addition of the RNase P protein to a precursor form of the P RNA in vitro results in autolytic processing of the 5′ and the 3′ end of this precursor in a matter of minutes. Autolytic processing produces the reported 5′ end of the mature P RNA. The precise 3′ end generated by autolytic processing is different over the course of the reaction and the final product is 4 nt shorter than the reported 3′ end of the *B. subtilis* P RNA. The observed 3′ end in vitro is consistent with the property of the holoenzyme reaction with single-stranded RNA substrates. The discrepancy with the reported 3′ end may be due to other processing events in vivo or inaccurate determination of the mature 3′ end of the P RNA isolated from the cell. We propose that the mature *B. subtilis* P RNA is generated at least in part by autolytic processing upon the binding of the RNase P protein to the precursor P RNA.

Keywords: holoenzyme; minimal substrate; P RNA; processing; RNase P

INTRODUCTION

RNase P is an essential endo-nuclease involved in producing the mature 5′ end of all tRNA in vivo. The bacterial RNase P is composed of a large RNA of 330-420 nt (denoted P RNA) and a small protein of ~120 amino acids (denoted P protein; Frank & Pace, 1998; Altman & Kirsebom, 1999). The in vitro reconstituted complex of P RNA and P protein, termed the holoenzyme, is a near-perfect enzyme, that is, the k_{cat}/K_m of cleaving the precursor tRNA substrate approaches the diffusion limited rates (Albery & Knowles, 1976; Kurz et al., 1998). In contrast, the k_{cat}/K_m of the catalyzed reaction of P RNA alone is $\sim 10^4$-fold lower under physiological conditions (Kurz et al., 1998).

A precursor tRNA substrate has a single-stranded RNA on the 5′ side of the cleavage site. A portion of the 5′ leader (nt −4 to −8) binds directly to a well-defined site in the P protein (Crary et al., 1998; Niranjanakumari et al., 1998b; Stams et al., 1998). Nucleotides −3 to −1 in the 5′ leader likely interact with the P RNA, both in the presence and in the absence of the P protein (Holm & Krupp, 1992; Smith & Pace, 1993; LaGrandeur et al., 1994; Crary et al., 1998; Loria et al., 1998, Christian & Harris, 1999). The tRNA portion of the substrate directly interacts with the P RNA (Harris et al., 1994; Pan et al., 1995; Loria et al., 1998; Massire et al.,

Reprint requests to: Tao Pan, Department of Biochemistry and Molecular Biology, University of Chicago, Chicago, Illinois 60637, USA; e-mail: taopan@midway.uchicago.edu.

Abbreviations: Holoenzyme: the 1:1 complex of the P RNA and the P protein; $K_{1/2}$: the ribozyme concentration at $k_{cl}/2$; k_{cl}: the cleavage rate at saturating ribozyme concentrations under single turnover conditions, that is, $[E] \gg [S]$; K_d: the dissociation constant of the ribozyme–substrate complexes; P protein: the RNase P protein from *Bacillus subtilis*; P RNA: the RNase P RNA component from *Bacillus subtilis*; Pre-P 1: A precursor form of P RNA containing 17 extra nt to the mature 5′ end and 90 extra nt to the reported mature 3′ end; Pre-P 2: A precursor form of P RNA containing the mature 5′ end and 90 extra nt to the reported mature 3′ end.

1998). Numerous studies have shown that RNase P primarily interacts with the T stem-loop and the acceptor stem portion of the tRNA (McClain et al., 1987; Kahle et al., 1990; Thurlow et al., 1991; Harris et al., 1994; Massire et al., 1998). Other studies have shown that deletion of the anticodon and the D stem-loops of a tRNA has little effect on the reaction catalyzed by the *Escherichia coli* RNase P holoenzyme (McClain et al., 1987).

As an RNase P substrate, the tRNA can be envisioned to be divisible into four components. The first component is a single-stranded RNA. The second component is an acceptor stem mimic that can be represented by a hairpin loop. The T stem-loop is added to mimic the coaxially stacked top portion of the tRNA. Inclusion of the anticodon and the D stem-loops reconstitutes the entire tRNA.

This work aims to elucidate the quantitative effects on catalytic efficiency and specificity of the *Bacillus subtilis* holoenzyme reaction upon the successive addition of RNA structures on the 3′ side of the cleavage site. In the course of this study, we realized that the cleavage efficiency of a single-stranded substrate is sufficiently high to consider the possibility of autolytic processing of the RNase P RNA precursors (pre-P RNA) in vivo upon P protein binding to the pre-P RNA. Indeed, an in vitro transcript containing extra nucleotides 5′ and 3′ to the mature P RNA is processed upon the addition of the P protein to produce precise 5′ and 3′ ends in a matter of minutes.

RESULTS

Design of RNA substrates

The RNA substrates are designed to incrementally increase the efficiency and specificity for the holoenzyme reaction. The simplest RNA substrate is a single-stranded RNA containing a 5′ leader region and a single nucleotide 3′ to the intended cleavage site (Fig. 1, substrate 1). Seven nucleotides are included in the 5′ leader region to allow optimal interaction with the 5′ leader-binding site in the P protein (Niranjanakumari et al., 1998b). The sequence of these 7 nt is composed entirely of adenosines and uridines to mimic the 5′ leader region of many natural tRNA substrates (Wawrousek et al., 1984; Green et al., 1985). Substrate 2 contains 2 additional nt at the 3′ end of substrate 1. The addition of these 2 nt may enable interactions between the region immediately 3′ to the cleavage site with the ribozyme.

The next substrate is designed with a hairpin loop 3′ to the cleavage site, mimicking the acceptor stem of a pre-tRNA substrate (substrate 3). The discriminator base in a pre-tRNA substrate is represented by the single nucleotide present at the 3′ end of this hairpin. Substrate 4 contains the CCA nucleotides at the extreme 3′ end, mimicking the conserved 3′CCA in a pre-tRNA substrate. The importance of the 5′ leader interaction with the P protein in the context of the hairpin-loop substrate is tested by deleting the 4 5′ most nt (substrates 5 and 6) in these substrates.

The natural pre-tRNA substrates (substrates 7 and 8) have the additional T stem-loop component in the context of the full-length tRNA. These substrates differ in the length of their 5′ leader to test the effect of the 5′ leader interaction with the holoenzyme in the context of the tRNA substrate.

Reaction kinetics

All substrates can be cleaved by the holoenzyme specifically to produce one major product (Figs. 1 and 2). Except for substrate 1, the cleavage site for all other substrates is the same as predicted in our design. No reaction products are observed when these substrates are incubated with the P protein in the absence of the P RNA (Fig. 2A and data not shown). The major cleavage site for substrate 1 is located at 1 nt 5′ to the intended cleavage site, whereas the minor cleavage site for this substrate is located at the designed position. The choice of these cleavage sites is probably due to competitive interaction between the different single-stranded segments 5′ and 3′ to the cleavage site with the holoenzyme. For the major cleavage site, the 3′ interaction involves 2 nt. Such 3′ interaction, in the context of substrate 1, appears to be stronger than the general guanosine preference for the nucleotide immediately 3′ to the cleavage site (Kirsebom, 1995; Loria et al., 1998). This guanosine preference is probably responsible for the observed minor cleavage site. Our results clearly indicate that holoenzyme is capable of cleaving substrates ranging from single-stranded RNA to tRNA precursors.

Two parameters are determined to quantitatively evaluate the cleavage efficiency and substrate binding under single turnover conditions, that is, $[E] \gg [S]$ (Table 1).

$$E + S \underset{k_{-1}}{\overset{k_1}{\rightleftarrows}} ES \xrightarrow{k_{cl}} EP.$$

We use k_{cl} here because the observed cleavage rate at a saturating RNase P concentration is believed to be a composite of two steps, one involving a fast equilibrium between two *ES* complexes and the other involving the actual chemical step, k_2 (Loria & Pan, 1999). We expect k_{cl} to be comparable to k_2 for the *B. subtilis* holoenzyme cleaving a pre-tRNA^{Asp} substrate ($\sim$20 min^{-1} at pH 6.1 in 10 mM $MgCl_2$ and 100 mM NH_4Cl) previously determined by Fierke and coworkers (Kurz et al., 1998). This value is indeed observed for the cleavage of our pre-tRNA^{Phe} substrate (Table 1). Deletion of the 5′ leader from 5 to 3 nt (compare substrates 7 and 8)

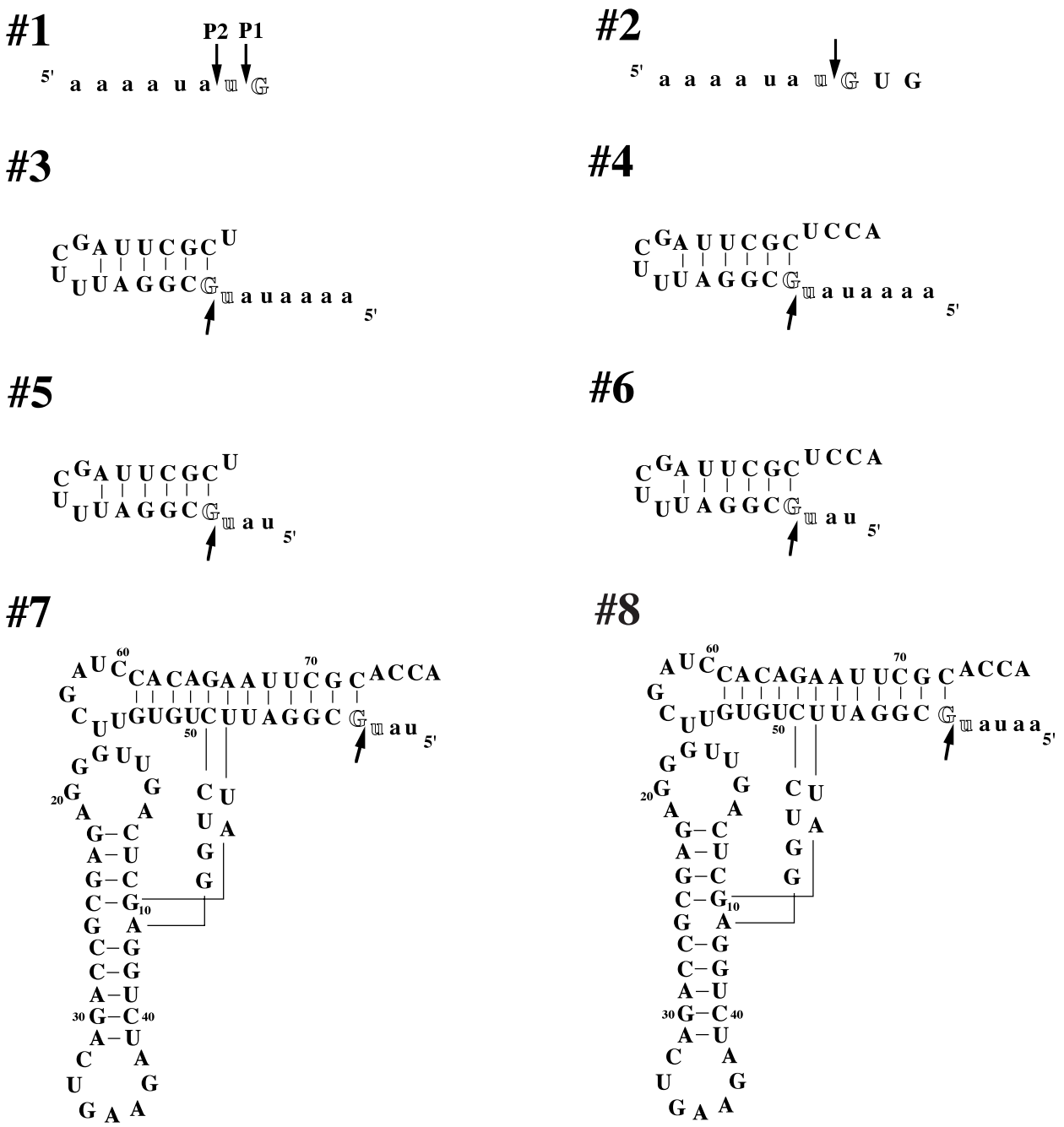

FIGURE 1. RNA substrates with the 5′ leader region shown in lower case. The designed cleavage sites are between the two highlighted residues. The observed cleavage sites are indicated by arrows.

does not change k_{cl}, similar to that observed for the holoenzyme cleavage of a pre-tRNA^{Asp} substrate (Crary et al., 1998). The manually measured k_{cl} for three representative substrates is pH dependent (Fig. 3A). A slightly greater slope (1.0) is observed for the single-stranded substrate 2 compared to the hairpin-loop substrate 4 (0.7).

The magnitude of the cleavage rate varies significantly for these substrates (Table 1). For single-stranded RNAs, extension of the 3′ region from a single nucleotide G to 3 nt GUG results in ~110-fold faster cleavage (compare the minor cleavage product P1 of substrate 1 to substrate 2). Substitution of the single-stranded 3′ region by a hairpin loop increases the cleavage rate by ~70-fold at pH 7.8 (compare substrate 2 to substrate 3) and up to ~ 600-fold at pH 5.9 (compare substrate 2 to 4, Fig. 3A). Addition of 3′ CCA to the hairpin loop improves the cleavage rate by ~1.5-fold when the 5′ leader has 7 nt (compare substrates 3 and 4). In the context of the hairpin-loop substrate, the 5′ leader can be reduced to 3 nt with less than fivefold effect on the cleavage rate (compare substrates 5/6 to

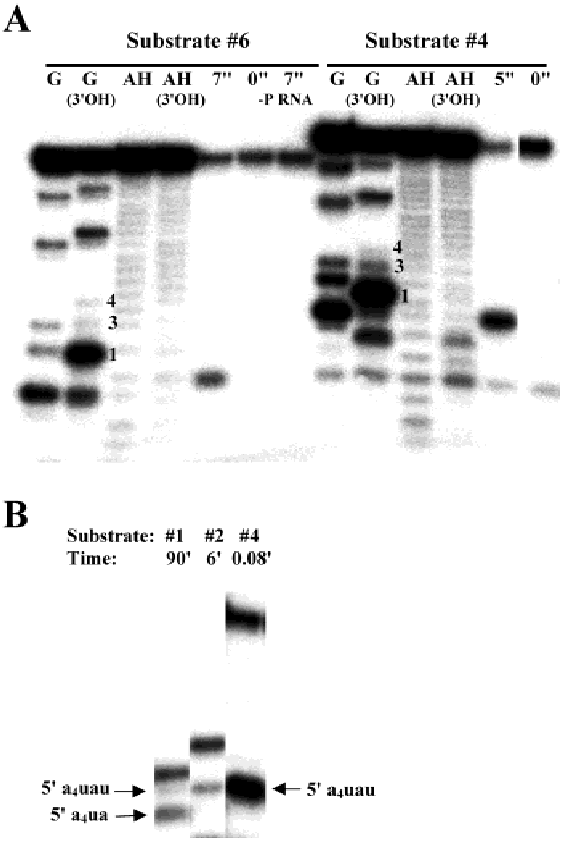

FIGURE 2. Identification of cleavage products by denaturing gel electrophoresis. **A**: The cleavage products of substrates 4 and 6 are compared to the partial alkaline hydrolysis and nuclease T1 digestion treated with a phosphatase (1 U/μL T4 polynucleotide kinase at 37 °C for 40 min) to remove the 2′, 3′ cyclic phosphate (Pan et al., 1995). AH, G: alkaline hydrolysis and T1 digestion in the absence of phosphatase. AH(3′OH), G(3′OH): alkaline hydrolysis and T1 digestion in the presence of phosphatase. The time points (in seconds) for the reaction (50 mM Tris-HCl, pH 7.78, 10 mM $MgCl_2$, 2% glycerol, 1 μM holoenzyme) are indicated. **B**: The cleavage products of substrates 1, 2, and 4 are compared. The time points (in minutes) for the reaction (50 mM Tris-HCl, pH 7.78, 10 mM $MgCl_2$, 2% glycerol, 1 μM holoenzyme) are indicated.

3/4). Replacing the hairpin loop with the entire tRNA increases the cleavage rate by another ~8-fold (compare substrates 4 and 8).

These results suggest that compared to a single-stranded RNA, the cleavage rate is mostly affected by the region 3′ to the cleavage site in the substrate. This interpretation is consistent with the previous observation that a series of pre-$tRNA^{Asp}$ substrates having 2–33 nt in the 5′ leader have essentially the same cleavage rate in the holoenzyme reaction (Crary et al., 1998). Similar to the pre-$tRNA^{Asp}$ and pre-$tRNA^{Phe}$ (Table 1) substrates, the effect on the cleavage rate of 5′ leader deletion in the context of the hairpin-loop substrate is small, especially in the presence of the 3′ CCA (compare substrates 4 and 6).

The ribozyme concentration at half-maximal cleavage rate, $K_{1/2}$, is defined as $(k_{-1} + k_{cl})/k_1$ where k_{-1} and k_1 are the off and on rate for substrate binding, respectively. $K_{1/2}$ can be used to approximate the substrate dissociation constant, $K_d = k_{-1}/k_1$ when $k_{-1} \gg k_{cl}$. Pulse-chase experiments are carried out to determine whether the $k_{-1} \gg k_{cl}$ condition is fulfilled for the substrates used in this work (Fig. 3B,C). In this experiment, the cleavage reaction under $[E] \gg [S]$ is allowed to proceed in the absence of a chase molecule to the extent that the majority of the substrate is bound to the enzyme. Upon the addition of a chase molecule, the free enzyme binds to the chase and is no longer available for binding of the substrate that dissociates from the pre-formed enzyme–substrate complex. When the substrate dissociation constant is much greater than the cleavage rate, that is, $k_{-1} \gg k_{cl}$, much less product will be generated in the presence of a chase molecule compared to the control where only the buffer and $MgCl_2$ are added. This result is observed for substrate 2 (Fig. 3B), suggesting that the holoenzyme reactions for the single-stranded substrates have significantly faster k_{-1} than k_{cl} under our conditions. Therefore, the dissociation constant of the ribozyme–substrate complex, K_d, can be approximated by the $K_{1/2}$ values for the single-stranded substrates to be 7–10 μM (Table 1).

In contrast, substrate 4 is cleaved to the same extent regardless of the addition of the chase molecule (Fig. 3C), suggesting that the holoenzyme reactions for the hairpin-loop substrates have faster k_{cl} than k_{-1} under our conditions. Fierke and coworkers have already shown that the holoenzyme reactions for pre-tRNA substrates have faster k_{cl} than k_{-1} (Kurz et al., 1998). Therefore, K_d for the hairpin loop and pre-tRNA substrates is lower than the $K_{1/2}$ values.

TABLE 1. Effects of successive addition of 3′ components in the *B. subtilis* RNase P holoenzyme reaction.

Substrate	k_{cl} (min^{-1})[a]	$K_{1/2}$ (μM)[b]
1[c]	0.038 ± 0.002 (P2) 0.0054 ± 0.0007 (P1)	7.0 ± 0.8
2	0.58 ± 0.05	9.5 ± 1.9
3	40 ± 5	2.5 ± 0.6
4	59 ± 13	1.4 ± 0.7
5	6.6 ± 0.6	6.2 ± 1.4
6	28 ± 2	4.5 ± 0.7
7[d]	23 ± 2	0.34 ± 0.07
8	16 ± 2	0.22 ± 0.05

[a]Cleavage rate at saturating enzyme concentration under single turnover conditions.
[b]The enzyme concentration for cleavage rate equal to $k_{cl}/2$.
[c]Conditions for substrate 1–6: 50 mM Tris-HCl, pH 7.78; 10 mM $MgCl_2$, 2% glycerol, 37 °C.
[d]Conditions for substrates 7–8: 50 mM MES, pH 5.88; 10 mM $MgCl_2$, 2% glycerol, 37 °C.

Autolytic processing of P RNA precursors in vitro

We have shown that the holoenzyme can effectively and specifically cleave a single-stranded RNA sub-

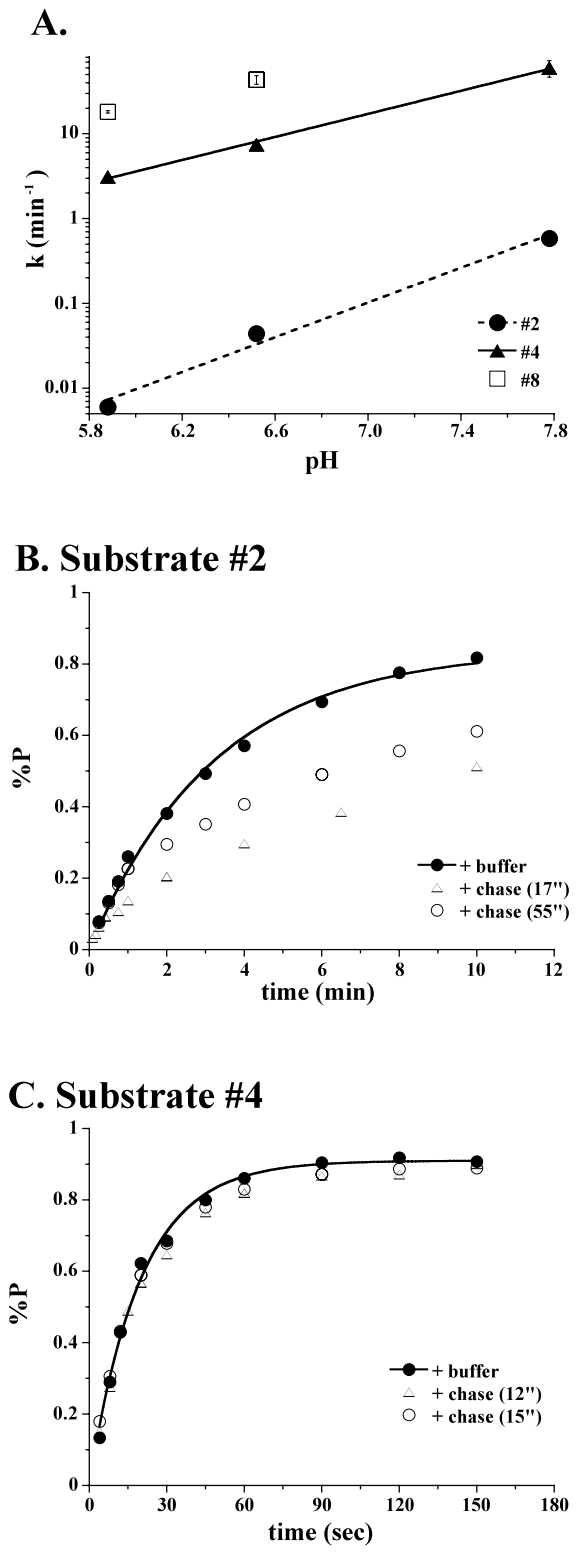

FIGURE 3. **A**: pH titration of the cleavage reaction at saturating holoenzyme concentrations for substrates 2 and 4. The cleavage rates of substrate 8 are also shown for comparison. **B**,**C**: Pulse-chase experiments to determine whether $k_{-1} \gg k_{cl}$ for substrates 2 (20 μM holoenzyme, $\sim 2 \times K_{1/2}$, 50 mM Tris-HCl, pH 7.78, 10 mM $MgCl_2$, 2% glycerol) and 4 (10 μM holoenzyme, $\sim 7 \times K_{1/2}$, 50 mM MES, pH 5.88, 10 mM $MgCl_2$, 2% glycerol). An *E. coli* tRNA mixture at a final concentration of 68 μM was used as the chase molecule (+ chase). Only buffer and $MgCl_2$ (+ buffer) were added in the control reactions.

strate at $\sim$0.6 min^{-1} at pH 7.8. Catalysis at this rate is comparable to many other RNA processing reactions observed in vitro and suggests the possibility for autolytic processing of P RNA transcript in vivo. Bacterial P RNA transcripts generally contain additional nucleotides at the 5′ end (Reich et al., 1986; Lee et al., 1989; Lundberg & Altman, 1995) and the 3′ end (Reed et al. 1982; Gurevitz et al., 1983; Reich et al., 1986; Lundberg & Altman, 1995; Kim et al., 1999). Which cellular component is involved in the processing of P RNA precursors is still unclear. Several reports suggest that *E. coli* RNase E may be involved in the processing of the *E. coli* RNase P RNA precursor (Gurevitz et al., 1983; Lundberg & Altman, 1995; Kim et al., 1999). To our knowledge, this is the first report to suggest that the precursors of the P RNA are processed autolytically in the presence of the P protein.

To test whether autolytic processing is feasible, two *B. subtilis* P RNA precursors were designed that mimic the in vivo transcripts of this P RNA. Both constructs contain 90 nt 3′ to the reported mature 3′ end of the *B. subtilis* P RNA (nt 401, from Reich et al., 1986). A putative transcriptional terminator hairpin is present within these 90 nt. The constructs differ in their 5′ end, reflecting the uncertainty of the 5′ end of the cellular transcripts of *B. subtilis* P RNA (Reich et al., 1986). The first construct (pre-P 1) contains 17 nt 5′ to the mature P RNA, whereas the second construct (pre-P 2) has the 5′ end of the mature P RNA. Both RNAs are made by T7 RNA polymerase transcription and purified by denaturing gel electrophoresis. The transcripts are renatured with Mg^{2+}. Autolytic processing in vitro is initiated by the addition of an equal-molar amount of the P protein.

Autolytic processing of the P RNA precursors is efficient and specific (Fig. 4). At 0.2 μM P RNA precursor + P protein, processing occurs within minutes at 3 or 10 mM $MgCl_2$. The final reaction product (band 4) is stable for at least 60 min. Two major processing intermediates (bands 2 and 3) can be observed. Kinetic analysis (data not shown) shows that both intermediates arise from faster processing at the 3′ end ($k_{obs} \sim$ 0.6 min^{-1} compared to $\sim$ 0.2 min^{-1} at the 5′ end at 10 mM $MgCl_2$), so that P RNA precursors with extra 5′ nucleotides accumulate.

The 5′ end of the in vitro processed P RNA (band 4) is determined by run-off reverse transcription using the band 4 RNA isolated by denaturing gel electrophoresis (Fig. 5A). Comparison to the sequencing lanes and to the run-off product of pre-P 2 shows that the band 4 RNA has a unique 5′ end identical to that of the mature P RNA. This result demonstrates that autolytic processing can produce the mature 5′ end of the *B. subtilis* P RNA.

The 3′ end of the in vitro processed P RNA (band 4) is analyzed first by labeling the band 4 product with [^{32}P]pCp with T4 RNA ligase, followed by partial (data

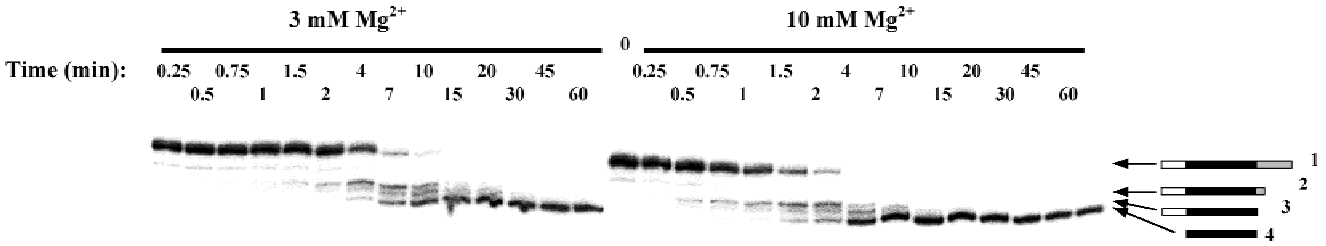

FIGURE 4. Autolytic processing of a P RNA precursor (pre-P 1) in the presence of the P protein at 37 °C. The reaction was carried out at 0.2 μM pre-P RNA + 0.2 μM P protein in 50 mM Tris-HCl, pH 8, 3 or 10 mM $MgCl_2$. The reaction times (in minutes) are indicated. Band 1 is the starting precursor containing extra nucleotides 5′ (open boxes) and 3′ (shaded boxes) to the mature P RNA (filled boxes). Band 4 is the end product of the processing reaction. Bands 2 and 3 are processing intermediates that still contain the 5′ region of the precursor.

not shown) and complete (Fig. 5B) nuclease T1 digestion. The T1 digestion products are compared to a synthetic RNA oligonucleotide comprised of nt 392–401 of the *B. subtilis* P RNA. Band 4 RNA can be efficiently labeled with [^{32}P]pCp, consistent with the generation of a 3′ hydroxyl group in an RNase P-catalyzed reaction. To our surprise, the 3′ end of the processed P RNA is heterogeneous, and the major product after 30 min incubation has a 3′ end at nt 397, not the reported nt 401. Although a product with the 3′ end at 401 is present, it never becomes a major product during the course of the reaction. There are two possible interpretations for this discrepancy. In one scenario, the mature P RNA in the cell has the 3′ end at nt 401. This scenario requires

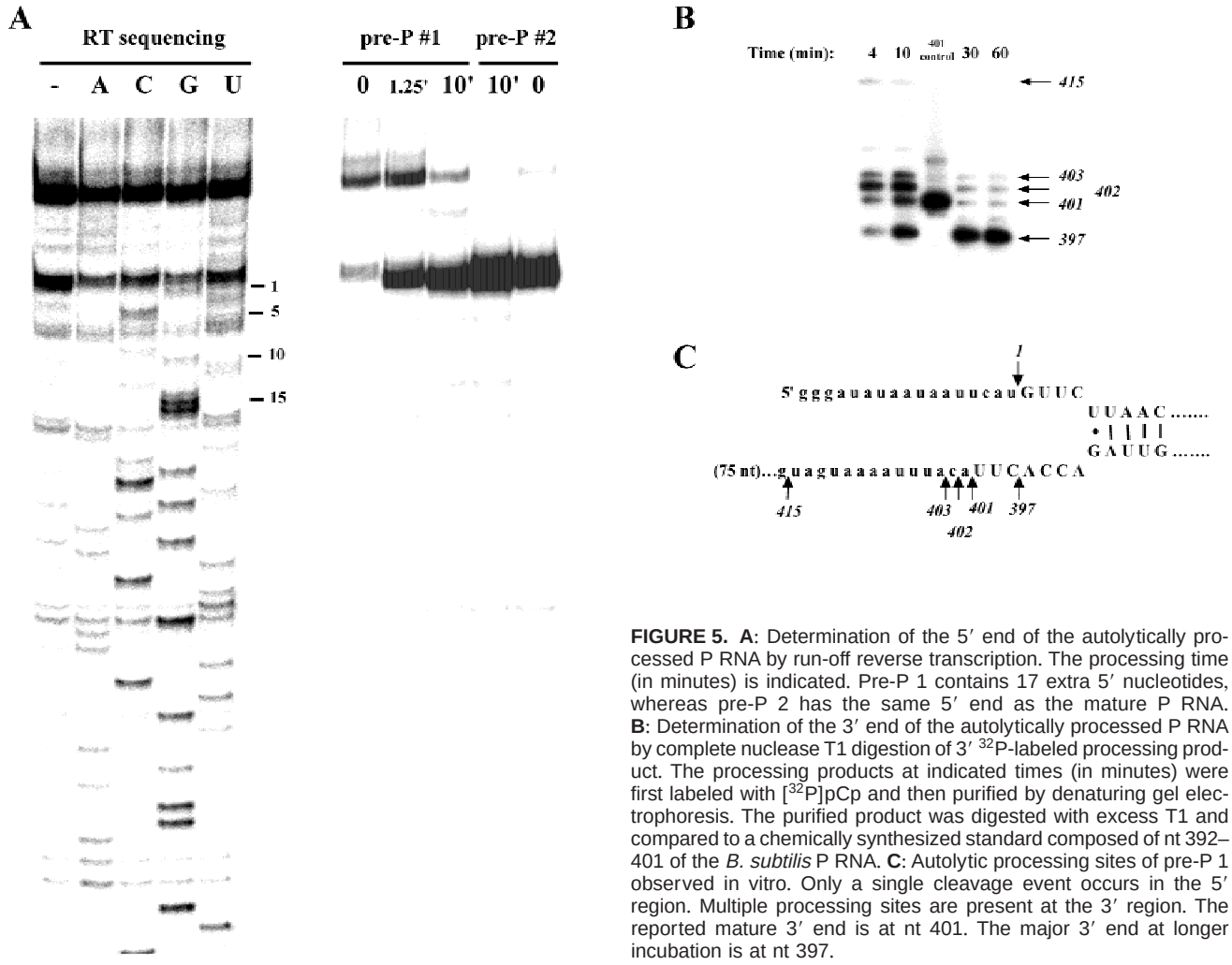

FIGURE 5. **A**: Determination of the 5′ end of the autolytically processed P RNA by run-off reverse transcription. The processing time (in minutes) is indicated. Pre-P 1 contains 17 extra 5′ nucleotides, whereas pre-P 2 has the same 5′ end as the mature P RNA. **B**: Determination of the 3′ end of the autolytically processed P RNA by complete nuclease T1 digestion of 3′ ^{32}P-labeled processing product. The processing products at indicated times (in minutes) were first labeled with [^{32}P]pCp and then purified by denaturing gel electrophoresis. The purified product was digested with excess T1 and compared to a chemically synthesized standard composed of nt 392–401 of the *B. subtilis* P RNA. **C**: Autolytic processing sites of pre-P 1 observed in vitro. Only a single cleavage event occurs in the 5′ region. Multiple processing sites are present at the 3′ region. The reported mature 3′ end is at nt 401. The major 3′ end at longer incubation is at nt 397.

either processing by another enzyme or autolytic processing in the presence of other cellular components. An alternative scenario is that the 3′ end of the mature *B. subtilis* P RNA in vivo is either heterogeneous or really corresponds to nt 397. In the single study that reported the 3′ end at nt 401 (Reich et al., 1986), the 3′ end of the purified cellular P RNA was also analyzed in the same fashion as described here, first labeling with [^{32}P]pCp, then partial alkaline hydrolysis and nuclease digestion. The sequence of the six 3′ nucleotides was presented as YYAYYn (Y = pyrimidine). However, the original data was not shown. Interestingly, the processed P RNA with a 3′ end at nt 397 has the 3′ sequence of AGAYYn, which is identical to the four 3′ most nucleotides in the original analysis.

DISCUSSION

Stepwise increase in the RNase P reactivity

The effect of four successive 3′ additions of structure/sequence to an RNA substrate for the *B. subtilis* holoenzyme reaction is summarized in Figure 6. Starting from the substrate with a single nucleotide 3′ to the cleavage site, the major increase in the cleavage rate is seen in the addition of two more single-stranded nucleotides followed by the addition of a hairpin loop. Each of the two additions improves the cleavage efficiency by about two orders of magnitude or 2.5–3.0 kcal/mol. Subsequent addition of the remainder of the tRNA component, the 3′ CCA and the T stem-loop region, only improves the cleavage rate by ~10-fold or 1.4 kcal/mol. The large effects on the cleavage rate do not strictly correlate with the gain in the binding affinity. Addition of more single-stranded nucleotides has no effect on substrate binding. These results demonstrate that cleavage efficiency and binding affinity for a holoenzyme substrate can be dictated by different 3′ components to the cleavage site.

Similar to our results on the 3′ components, Fierke and coworkers showed that the cleavage efficiency and binding affinity are dictated by different nucleotides in the 5′ leader as well (Crary et al., 1998). In the context of pre-tRNA^{Asp}, substrates with 5′ leaders ranging from 2 to 33 nt have the same cleavage rate constant. The major improvement in cleavage chemistry results from increasing the 5′ leader from 1 to 2 nt. Substrate binding, on the other hand, is improved in two major steps. These steps involve increasing the 5′ leader from 1 to 2 nt and from 4 to 5 nt. Fierke and coworkers (Crary et al., 1998) proposed that the first gain in the cleavage chemistry and in the binding affinity is due to interaction of the −2 nt with the P RNA. The second improvement in the binding affinity is due to direct interaction of the −5 nt with the P protein. These previous and present results indicate that cleavage rate and binding affinity for the holoenzyme reaction can be gained in major steps by the addition of RNA segments

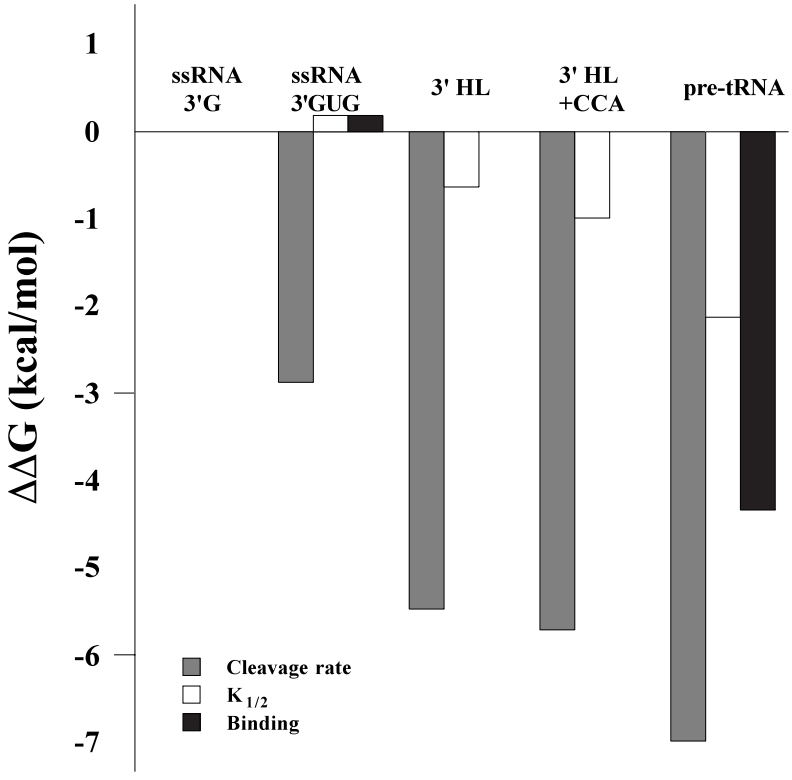

FIGURE 6. Improvement of the cleavage rate and substrate binding upon the successive addition of RNA structure/nucleotides 3′ to the cleavage site. The ΔΔG values are normalized to the cleavage site P1 of substrate 1. The data point for the K_d of the holoenzyme–tRNA substrate is taken from a pre-tRNA^{Asp} with 33 nt in the 5′ leader determined by Kurz et al. (1998).

to either end of a minimal substrate. The quantitative interplay between holoenzyme interaction with the 5′ or the 3′ region of the substrate is, however, quite complex and not fully understood.

Minimal RNA substrate for the RNase P holoenzyme

The *B. subtilis* RNase P holoenzyme can accurately cleave a single-stranded RNA substrate at a rate of ~0.6 min^{-1} at pH 7.8. This cleavage rate is comparable to the cleavage rate observed for small ribozymes such as the hammerhead ribozyme (Hertel et al., 1994). The holoenzyme reaction for a single-stranded RNA substrate has a $K_{1/2}$ of 7–10 μM, resulting in a k_{cat}/K_M value of ~10^5 M^{-1} min^{-1}. This value is ~2,000-fold lower than the k_{cat}/K_M for the holoenzyme reaction for a pre-tRNA substrate (Kurz et al., 1998; unpubl. result). The optimal cleavage efficiency requires the presence of more than 1 nt 3′ to the cleavage site, even though the binding affinity does not change for single-stranded substrates with additional 3′ nucleotides. The increase in the cleavage rate may be the result of substrate destabilization induced by the interaction between the holoenzyme and these additional 3′ nucleotides (Beebe & Fierke, 1994; Narlikar & Herschlag, 1998). This same effect would obliterate a potential increase in the binding affinity.

Autolytic processing of P RNA in the presence of the P protein

The efficiency of the holoenzyme reaction for a single-stranded RNA substrate (~0.6 min^{-1}) inspires us to consider the possibility of autolytic processing of the P RNA transcript. The autolytic processing events have half-lives of 1–3 min at 0.2 μM P RNA precursor + 0.2 μM P protein under our in vitro condition (10 mM $MgCl_2$, pH 8, 37 °C). Autolytic processing in vitro also produces the precise 5′ end of the mature P RNA. Data presented for the identification of the mature 3′ end in vivo (Reich et al., 1986) are insufficient to invalidate our proposal of autolytic processing in the generation of the mature 3′ end of the P RNA.

A comprehensible model for the *B. subtilis* P RNA maturation can be proposed by combining the results for the single-stranded RNA substrates and the observed autolytic processing in vitro (Fig. 7). This model assumes that the 5′ and 3′ autolytic processing events are independent, as supported by the comparable 3′ processing rates for P RNA precursors containing either 0 or 17 extra 5′ nucleotides. Upon the formation of a pre-P RNA/P protein complex, about 80–90% of the P RNA precursor undergoes an initial 3′ processing to produce a second precursor with the 3′ end at nt 415 (major pathway in Fig. 7). This second precursor is either 3′ processed or 5′ processed in two consecutive steps to produce a third P RNA that contains the mature 5′ end, but with a heterogeneous 3′ end at nt 401, 402, or 403. This third P RNA can be further processed to produce a stable product with the 3′ end at nt 397. The other 10–20% of the precursor undergoes 5′ processing to produce the mature 5′ end first (minor pathway in Fig. 7). This new precursor is further processed as outlined for the processing of the major P RNA fraction.

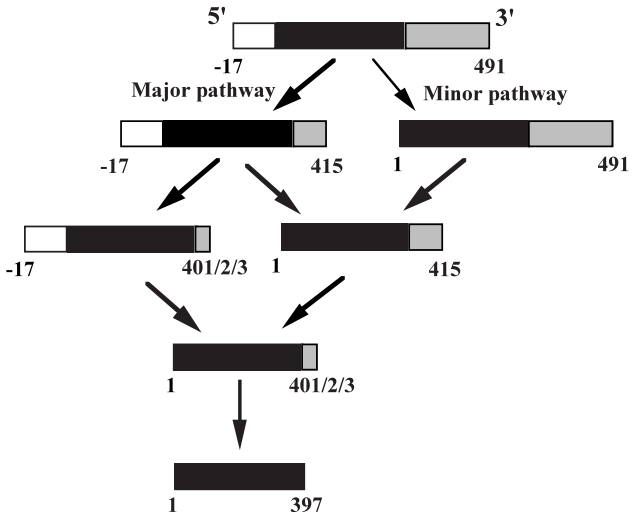

FIGURE 7. In vitro observed autolytic processing pathway. The 5′ and 3′ precursor regions are shown as an open and a shaded box, respectively. The end product of the processed P RNA is shown as a filled box. The terminal nucleotides at each stage of the processing reaction are indicated.

What properties of the holoenzyme prevent further processing of the 5′ and 3′ ends of a mature P RNA? We have found recently that P protein binding protects several 5′ nucleotides in the P RNA against the hydroxyl radical attack (unpubl. results). The mature 5′ end of P RNA is proposed in the structural models to be proximal to one other protected region in the P8/P9 helical junction (Harris et al., 1994; Chen et al., 1998; Massire et al., 1998). Three potential RNA binding sites in the P protein have been proposed from its crystal structure (Stams et al., 1998). One of the two sites has been confirmed by UV crosslinking to bind the −4 to −8 nt in the 5′ leader of a tRNA substrate (Niranjanakumari et al., 1998b). It is therefore likely that the P protein may directly contact the P8/P9 region and several 5′ nucleotides in the mature P RNA. P protein binding in the region close to the 5′ end could prevent the 5′ end of the P RNA from further processing by RNase P or other cellular nucleases.

Reaction kinetics of single-stranded RNA substrates by the holoenzyme may explain the processing sites observed at the 3′ end. Processing at nt 415 is consistent with the preference of a 3′ guanosine in single-stranded RNA substrates. The most efficient

single-stranded RNA substrate contains at least 7 nt in the 5′ leader, because P protein binds to −4 to −8 nt. This requirement is satisfied for cleavage at the nt 401/402/403. Cleavage at nt 397 may only be possible upon transient opening of helix P1 that would provide 7 unpaired nt to function as a 5′ leader.

MATERIALS AND METHODS

RNA Preparation

The *B. subtilis* P RNA was prepared by the standard in vitro transcription method using T7 RNA polymerase (Milligan & Uhlenbeck, 1989). The single-stranded and hairpin-loop substrates were chemically synthesized using 2′ ortho–ester-protected phosphoramidites (Dharmacon Research, Boulder, Colorado). The pre-tRNA substrates were prepared by enzymatic ligation (Moore & Sharp, 1992) of a synthetic oligonucleotide to an RNA transcript composed of nt 10–76 of the yeast $tRNA^{Phe}$ (Loria & Pan, 1997). The *B. subtilis* P protein was prepared from an overexpression clone as described by Fierke and coworkers (Niranjanakumari et al., 1998a).

P RNA precursors

Two constructs were made to mimic the precursor form of the *B. subtilis* P RNA in vivo. Construct 1 (pre-P 1) contains all residues of the mature P RNA with 17 nt added to the 5′ end and 90 nt added to the 3′ end. Fourteen of the 17 extra nt at the 5′ end are the natural sequence 5′ to the mature P RNA. Three Gs were added to improve transcription. All 90 extra nt at the 3′ end correspond to the natural sequence 3′ to the mature P RNA. Construct 2 (pre-P 2) has the 5′ end of the mature P RNA as well as the same 90 nt added to the 3′ end.

The transcription templates for the P RNA precursors were made by PCR using the *B. subtilis* genomic DNA prepared according to Wilson (1990). Both PCR reactions shared the same 3′ primer: 5′-CATCGTATCACCCTGT, but differed in their 5′ primers: 5′-TAATACGACTCACTATAGGGATATAATA ATTCATGTTC for pre-P 1 and 5′-TAATACGACTCACTATA GTTCTTAACGTTCGGGTA for pre-P 2.

Kinetics of the cleavage reaction

All reaction kinetics were performed under single turnover conditions at 0.02–25 μM enzyme and <2 nM of ^{32}P-labeled substrates. The holoenzyme was reconstituted as described previously (Loria et al., 1998). Briefly, P RNA in buffer was heated at 85 °C for 2 min, followed by incubation for 3 min at room temperature. Mg^{2+} was added to designated concentrations. The mixture was incubated for 5–10 min at 50 °C. An equal-molar ratio of P protein was added. The mixture was further incubated for 5 min at 37 °C. The 5′ ^{32}P-labeled RNA substrates were renatured as described previously (Loria & Pan, 1997). The cleavage reaction was initiated upon mixing an equal volume of the ribozyme and the substrate. Aliquots were taken at designated time points and mixed with an excess of 9 M urea/100 mM EDTA to stop the cleavage reaction. The reaction products were separated from the unreacted substrates on denaturing gels containing 7 M urea. The amount of products and substrates was determined by phosphorimaging using a Fuji Phosphorimager. The reaction rates were obtained by fitting the amount of cleavage products over time to a single exponential.

For autolytic processing, the P RNA precursors were first renatured as described above. The reaction was initiated upon the addition of the P protein. The reaction was stopped upon mixing with an excess of 9 M urea/100 mM EDTA, and was analyzed by denaturing gels containing 7 M urea.

Pulse-chase experiments were carried out as described previously for the holoenzyme reactions using the *E. coli* type XXI tRNAs as the chase (Beebe & Fierke, 1994; Loria et al., 1998) to test whether the rate of substrate dissociation, k_{-1}, was greater than the rate of cleavage at saturating ribozyme concentration, k_{cl}. The amount of enzyme was 20 μM ($\sim 2 \times K_{1/2}$) for substrate 2 and 10 μM ($\sim 7 \times K_{1/2}$) for substrates 4 and 8. Reaction with a trace amount of ^{32}P-labeled substrate was allowed to proceed for 12–55 s, at which time *E. coli* tRNA mixture was added to a final concentration of 68 μM ($K_i \sim 3$ μM for a pre-$tRNA^{Phe}$ substrate with a 2′ H at the cleavage site; Loria et al., 1998). Only buffer and $MgCl_2$ were added in the control reaction.

Mapping the 5′ and 3′ ends of autolytically processed P RNA

The 5′ end of the processed P RNA was determined by reverse transcription using a primer complementary to nt 47–61 or 71–85 of the mature P RNA. The reverse transcription was carried out using the gel-purified P RNA products under standard conditions as described by the manufacturer (Amersham, Inc.).

To determine the 3′ end of the processed P RNA, the P RNA product was first labeled with [^{32}P]pCp using T4 RNA ligase (England et al., 1980). The labeled products were purified by denaturing gel electrophoresis. A partial or a total T1 digest was carried out with the labeled products and reaction mixture compared to a synthetic oligonucleotide standard composed of the nt 392–401 of the P RNA. The partial T1 digest was performed with a trace amount of labeled RNA in the presence of 1 μg *E. coli* tRNA mixture and 1 U nuclease T1 at 65 °C for 1 min. The complete T1 digest was performed with a trace amount of labeled RNA only and 5 U nuclease T1 at 65 °C for 2 min.

ACKNOWLEDGMENTS

We thank Drs. Carol Fierke and S. Niranjanakumari for the generous gift of the overexpression plasmid for the P protein. We also thank Drs. C. Correll, N. Pace, T. Sosnick, and X.-W. Fang for helpful discussions and comments on the manuscript. This work was supported by a grant from the National Institutes of Health (GM52993). We thank both reviewers for their comments; in particular, we greatly appreciate the insightful comments of one reviewer on the reaction kinetics.

Received May 10, 2000; returned for revision
June 27, 2000; revised manuscript received July 11, 2000

REFERENCES

Albery WJ, Knowles JR. 1976. Evolution of enzyme function and the development of catalytic efficiency. *Biochemistry 15*:5631–5640.

Altman S, Kirsebom LA. 1999. Ribonuclease P. In Gesteland RF, Cech TR, Atkins JF, eds. *The RNA world*. Cold Spring Harbor, New York: Cold Spring Harbor Laboratory Press. pp 351–380.

Beebe JA, Fierke CA. 1994. A kinetic mechanism for cleavage of precursor $tRNA^{Asp}$ catalyzed by the RNA component of *Bacillus subtilis* Ribonuclease P. *Biochemistry 33*:10294–10304.

Chen JL, Nolan JM, Harris ME, Pace NR. 1998. Comparative photocrosslinking analysis of the tertiary structure of *Escherichia coli* and *Bacillus subtilis* RNase P RNAs. *EMBO J 17*:1515–1525.

Christian EL, Harris ME. 1999. The track of the pre-tRNA 5′ leader in the ribonuclease P ribozyme-substrate complex. *Biochemistry 38*:12629–12638.

Crary SM, Niranjanakumari S, Fierke CA. 1998. The protein component of *Bacillus subtilis* RNase P increase catalytic efficiency by enhancing interactions with the 5′ leader sequence of pre-$tRNA^{Asp}$. *Biochemistry 37*:9409–9416.

England TE, Bruce AG, Uhlenbeck OC. 1980. Specific labeling of 3′ termini of RNA with T4 RNA ligase. *Methods Enzymol 65*:65–74.

Frank DN, Pace NR. 1998. Ribonuclease P: Unity and diversity in a tRNA processing ribozyme. *Annu Rev Biochem 67*:153–180.

Green CJ, Stewart GC, Hollis MA, Vold BS, Bott KF. 1985. Nucleotide sequence of the *Bacillus subtilis* ribosomal RNA operon, rrnB. *Gene 37*:261–266.

Gurevitz M, Jain SK, Apirion D. 1983. Identification of a precursor molecular for the RNA moiety of the processing enzyme RNase P. *Proc Natl Acad Sci USA 80*:4450–4454.

Harris ME, Nolan JM, Malhotra A, Brown JW, Pace NR. 1994. Global architecture of the ribonuclease P RNA-pre tRNA complex. *EMBO J 13*:3953–3963.

Hertel KJ, Herschlag D, Uhlenbeck OC. 1994. A kinetic and thermodynamic framework for the hammerhead ribozyme reaction. *Biochemistry 33*:3374–3385.

Holm PS, Krupp G. 1992. The acceptor stem in pre-tRNAs determines the cleavage specificity of RNase P. *Nucleic Acids Res 20*:421–423.

Kahle D, Wehmeyer U, Krupp G. 1990. Substrate recognition by RNAse P and by the catalytic M1 RNA: Identification of possible contact points in pre-tRNAs. *EMBO J 9*:1929–1937.

Kim S, Sim S, Lee Y. 1999. In vitro analysis of processing at the 3′-end of precursors of M1 RNA, the catalytic subunit of *Escherichia coli* RNase P: Multiple pathways and steps for the processing. *Nucleic Acids Res 27*:895–902.

Kirsebom LA. 1985. RNase P: A “Scarlet Pimpernel.” *Mol Microbiol 17*:411–420.

Kurz JC, Niranjanakumari S, Fierke CA. 1998. Protein component of *Bacillus subtilis* RNase P specifically enhances the affinity for precursor-$tRNA^{Asp}$. *Biochemistry 37*:2393–2400.

LaGrandeur TE, Huttenhofer A, Noller HF, Pace NR. 1994. Phylogenetic comparative chemical footprint analysis of the interaction between ribonuclease P RNA and tRNA. *EMBO J 13*:3945–3952.

Lee Y, Ramamoorthy R, Park CU, Schmidt FJ. 1989. Sites of initiation and pausing in the *Escherichia coli* rnpB (M1 RNA) transcript. *J Biol Chem 264*:5098–5103.

Loria A, Niranjanakumari S, Fierke CA, Pan T. 1998. Recognition of a pre-tRNA substrate by the *Bacillus subtilis* RNase P holoenzyme. *Biochemistry 37*:15466–15473.

Loria A, Pan T. 1997. Recognition of the T stem-loop of a pre-tRNA substrate by the ribozyme from *Bacillus subtilis* ribonuclease P. *Biochemistry 36*:6317–6325.

Loria A, Pan T. 1999. The cleavage step of the ribonuclease P catalysis is determined by ribozyme–substrate interactions both distal and proximal to the cleavage site. *Biochemistry 38*:8612–8620.

Lundberg U, Altman S. 1995. Processing of the precursor to the catalytic RNA subunit of RNase P from *Escherichia coli*. *RNA 1*:327–334.

Massire C, Jaeger L, Westhof E. 1998. Derivation of the three-dimensional architecture of bacterial ribonuclease P RNAs from comparative sequence analysis. *J Mol Biol 279*:773–793.

McClain WH, Guerrier-Takada C, Altman S. 1987. Model substrates for an RNA enzyme. *Science 238*:527–530.

Milligan JF, Uhlenbeck OC. 1989. Synthesis of small RNAs using T7 RNA polymerase. *Methods Enzymol 180*:51–64.

Moore MJ, Sharp PA. 1992. Site-specific modification of pre-mRNA: The 2′ hydroxyl groups at the splice site. *Science 256*:992–997.

Narlikar GJ, Herschlag D. 1998. Mechanistic aspects of enzymatic catalysis: Lessons from comparison of RNA and protein enzymes. *Annu Rev Biochem 66*:19–59.

Niranjanakumari S, Kurz JC, Fierke CA. 1998a. Expression, purification and characterization of the recombinant RNase P protein component from *Bacillus subtilis*. *Nucleic Acids Res 26*:3090–3096.

Niranjanakumari S, Stams T, Crary SM, Christianson DW, Fierke CA. 1998b. Protein component of the ribozyme ribonuclease P alters substrate recognition by directly contacting precursor tRNA. *Proc Natl Acad Sci USA 95*:15212–15217.

Pan T, Loria A, Zhong K. 1995. Probing tertiary interactions in RNA: 2′OH-base contacts between the RNase P RNA and pre-tRNA. *Proc Natl Acad Sci USA 92*:12510–12514.

Reed RE, Baer MF, Guerrier-Takada C, Donis-Keller H, Altman S. 1982. Nucleotide sequence of the gene encoding the RNA subunit (M1 RNA) of ribonuclease P from *Escherichia coli*. *Cell 30*:627–636.

Reich C, Gardiner KJ, Olsen GJ, Pace B, Marsh TL, Pace NR. 1986. The RNA component of the *Bacillus subtilis* RNase P: Sequence, activity, and partial secondary structure. *J Biol Chem 261*:7888–7893.

Smith D, Pace NR. 1993. Multiple magnesium ions in the ribonuclease P reaction mechanism. *Biochemistry 32*:5273–5281.

Stams T, Niranjanakumari S, Fierke CA, Christianson DW. 1998. Ribonuclease P protein structure: Evolutionary origins in the translational apparatus. *Science 280*:752–755.

Thurlow DL, Shilowshi D, Marsh TL. 1991. Nucleotides in precursor tRNAs that are required intact for catalysis by RNAse P RNAs. *Nucleic Acids Res 19*:885–891.

Wawrousek EF, Narasimhan N, Hansen JN. 1984. Two large clusters with thirty-seven transfer RNA genes adjacent to ribosomal RNA gene sets in *Bacillus subtilis*. Sequence and organization of trrnD and trrnE gene clusters. *J Biol Chem 259*:3694–3702.

Wilson K. 1990. Preparation of genomic DNA from bacteria. In Ausubel FM, Brent R, Kingston RE, Moore DD, Seidman JG, Smith JA, Struhl K, eds. *Current protocols in molecular biology*. New York: Wiley Interscience. pp 2.4.1–5.